JOURNAL OF COMPUTATIONAL PHYSICS 75, 384–399 (1988)

Numerical Simulation of Cylindrically Converging Shock Waves

H. MATSUO, Y. OHYA,* AND K. FUJIWARA

Faculty of Engineering, Kumamoto University, Kumamoto, Japan

AND

H. KUDOH

Mazda Co. Ltd., Hiroshima, Japan

Received August 14, 1986; revised January 30, 1987

The converging shock wave is assumed to be generated by an instantaneous energy release on a rigid cylindrical wall. The fluid flow caused by its propagation is numerically simulated. The behavior of the solution in the focusing stage is closely investigated and compared with the selfsimilar solution. Results include new details of the transition of the solution from the nonselfsimilar region to the selfsimilar region. Numerical methods such as the random choice method, the method of characteristics, and the second-order accurate finite difference method with artificial viscosities are adopted. The results are also compared with those of the method of integral relations. They all agreed well with one another except for the focusing stage. The random choice method and the method of characteristics produce nearly identical results in the focusing stage, suggesting the mutual credibility of the two methods. Artificial viscosities involved in the finite difference scheme smear out the shock front as it approaches the axis. The comparison with the selfsimilar solution is then difficult.

I. INTRODUCTION

In this paper, the fluid flow caused by the propagation of a cylindrically converging shock wave is numerically simulated. The shock wave is assumed to be generated by an instantaneous energy release on a rigid cylindrical wall. The flow of this kind was first analyzed by Bach and Lee [1], and later by Matsuo [2–4]. The application of the Bach and Lee solution was limited to the initial propagation of the shock wave in close proximity to the wall. Using the method of integral relations, Matsuo obtained a "global solution," that is, a solution which describes the whole history of the fluid motion from the initial stage near the wall to the convergence stage near the axis. It was shown that as the wave propagates towards the axis, the solutions tend to approach but never reach the selfsimilar implosion limit

* Present address: Research Institute for Applied Mechanics, Kyushu University, Kasuga-Shi, Japan.

0021-9991/88 $3.00

[5]. The rate of approach appeared to be slower than expected. The application of the selfsimilar solution also appeared to be restricted to a very small region behind the front. As pointed out in Ref. [3], however, the convergence of the method of integral relations tends to deteriorate as the shock front approaches the region in close proximity to the axis. It has then been suggested that other numerical methods should be considered to investigate more closely the transition from the nonselfsimilar region to the selfsimilar region. Apart form the purely mathematical interest, the need for such an investigation has been increased in the engineering practice. Converging shock waves have been utilized there to produce an extreme condition of ultra-high temperature, density and pressure [6–8]. Indeed questions arise there: Does the flow actually fall within the selfsimilar regime before the shock front enters the region near the point of convergence where the fluid dynamics of nondissipative and electrically neutral continua may break down? If it does, what is the selfsimilar region and to what extent behind the shock front does it hold? The primary aim of the present study is to answer these questions. Several existing numerical methods are then compared to deduce the conclusion. However, more modern numerical methods incorporating finite differences such as those reviewed later [9–12] are not tested since the answer has been obtained without referring to them.

Numerical simulations of cylindrically converging shock waves have been made by several investigators. Most of them, however, have been restricted to the cylindrical shock tube problems with moderate initial pressure ratios. Sod [13] computed this problem by combining the Glimm's method [14] (the random choice method) and operator splitting. The sharp discontinuity was maintained throughout the calculation although it was a natural consequence considering the character of the method. Comparisons with the finite difference methods indicated that there was a difference in the time at which the shock reached the axis. Saito and Glass [15] applied this method to the implosion problem rather than the shock tube problem. In fact they treated the explosive-driven hemispherical converging shock wave. It was reported that reasonable results were obtained. The finite difference method was first applied to the cylindrical shock tube problem by Payne [16]. The Lax scheme was used and a plausible result was obtained. Lapidus [17] proposed the "Cartesian method" to compute flows with radial symmetry. The results were compared with Payne's solutions. Some differences including those in shock speeds were pointed out. Abarbanel and Goldberg [18] computed the same problem using an iterative procedure based on the Lax–Wendroff method. The result differed markedly from Payne's solutions. Very recently Ben-Artzi and Falcovitz [12] proposed an upwind second-order scheme based on the GRP (generalized Riemann problem) method. This method is unique in solving nonplanar flows without resorting to operator splitting. Cylindrical shock tube problems were tested and it was reported that the results, including the arrival time of the shock at the axis as well as the shape and extremal values of the flow profiles, were in very good agreement with those of Abarbanel and Goldberg [18] and Sod [13].

The problem which is to be treated here involves two distinct points. They are: (i) The initial pressure ratio is much larger than that in the preceding studies. Actually it ranges from tens to thousands, and (ii) the initial condition is not uniform along the space variable. The flow variables change abruptly behind the discontinuity. It seems that such situations were severe for the numerical simulation. Several preliminary calculations were then made for the plane and cylindrical shock tube problems to seek suitable numerical methods. Finally three methods were adopted; that is, the random choice method combined with operator splitting, the method of characteristics, and the second-order accurate finite difference methods with artificial viscosities.

The random choice method produced very favorable results. They agreed very well with the results of the method of integral relations [3, 4] except for the region in close proximity to the axis. It would be worth noting that two results obtained by different numerical methods agree with each other. This would imply the correctness of the two solutions. Near the axis, the solutions of the random choice method approach the selfsimilar solutions more quickly than those of the method of integral relations. However, the rate of approach is still slower than expected. In fact the selfsimilar solution begins to hold when the shock radius is less than 2% of the initiation radius. Even then, it only holds in a narrow region behind the front.

The result of the method of characteristics agreed well with the two previous solutions except for the focusing stage. In the region near the axis, it is nearly identical with that obtained by the random choice method. Considering the fact that the random choice method and the method of characteristics are based on distinctly different formulations, it seems to suggest the mutual credibility of the two methods. It also suggests that the conclusion deduced from the random choice method is correct.

It seemed that the situation associated with the initial conditions was particularly severe for the finite difference method. Several schemes were then tested with different artificial viscosities. Most of the calculations could not be rid of strong oscillation behind the discontinuity. They eventually led to instability. The most favorable result was obtained by the second-order schemes, particularly by the MacCormack scheme [19] with artificial diffusion terms. The result of calculations agreed well with the other three results, except for the region near the axis. In the focusing stage, it begins to differ from the others. The shock speed is slower and the discontinuity is smeared out due to viscosity. Small oscillations still remain behind the shock front. The comparison with the selfsimilar solutions is then difficult. However, it should be mentioned that difficulties encountered here do not imply the deficiency of finite difference methods. Rather, more modern methods incorporating finite differences would produce solutions with higher accuracy. In fact many advances have been made in the past few years in dealing with weak solutions to Euler's equations within the context of finite differences. Roe [9], for example, reviewed the recent progress in this area. Of all these works one may, for example, refer to works by Harten [10], Roe and Pike [11], and Ben-Artzi and Falcovitz [12].

One more thing to be remarked is the problem of the reflexion of shock waves from the axis. However, seeking the most reliable method for analyzing incoming waves is prerequisite to the study of the reflexion. Hence the present study will serve for the investigation in future.

II. Basic Equations and Initial Data

The conservation laws for the inviscid and nonconducting flow with cylindrical symmetry are written as

$$\frac{\partial U}{\partial t}+\frac{\partial F(U)}{\partial r}+W(U)=0, \tag{1}$$

with

$$U=\begin{pmatrix}\rho\\ \rho u\\ e\end{pmatrix}, \tag{2}$$

$$F(U)=\begin{pmatrix}\rho u\\ \rho u^2+p\\ u(e+p)\end{pmatrix}, \tag{3}$$

$$W(U)=\begin{pmatrix}\rho u/r\\ \rho u^2/r\\ u(e+p)/r\end{pmatrix}, \tag{4}$$

whereas t and r are the independent variables which represent the time and the space coordinate respectively; ρ, u, p, and e are, respectively, density, particle velocity, pressure and total energy per unit volume. Assuming polytropic gas, e is represented by

$$e=p/(\gamma-1)+\rho u^2/2, \tag{5}$$

where γ is the ratio of specific heats.

We shall now assume that the cylindrically converging shock wave is generated by an instantaneous release of the energy E per unit length of the cylinder at the rigid cylindrical surface $r=R_0$. Nondimensional variables are defined as

$$\begin{aligned}&\bar{p}=p/p_0, \qquad \bar{\rho}=\rho/\rho_0, \qquad \bar{u}=\sqrt{\gamma}u/c_0,\\ &\bar{c}=\sqrt{\gamma}c/c_0, \qquad \bar{r}=r/R_0, \qquad \bar{t}=c_0t/\sqrt{\gamma}R_0,\end{aligned} \tag{6}$$

where p_0, ρ_0, and c_0 are the pressure, the density, and the sound speed in undisturbed fluid, respectively. Equation (1) remains unchanged by the substitution of Eq. (6). Nondimensional quantities ξ and E_0 are defined for the later use as

$$\xi = (R_0 - R_s)/R_0, \tag{7}$$

$$E_0 = E/(2\pi p_0 R_0^2), \tag{8}$$

where R_s is the coordinate of the shock front.

The boundary condition at the cylindrical surface is written as

$$u = 0 \qquad \text{for} \quad r = R_0. \tag{9}$$

The perturbation solutions at $\xi = 0.1$ are used as the initial data of the random choice method and the finite difference method. They were originally obtained by Bach and Lee [1] and later recalculated by Matsuo [2]. In the calculation adopting the method of characteristics, the solutions at $\xi = 0.3$ obtained by the method of integral relations [3,4] are used as the initial data (see III. B). It was shown that the sound speed is infinite (density is zero) at the cylindrical wall $r = R_0$ [3, 4]. Some trick in the numerical procedure would be necessitated to cope with this difficulty. Zero density at the wall might be interpreted as follows: At the instant of energy deposition ($t = 0$), a shock wave of infinite strength is produced at the wall. This is the consequence of the analysis which neglects dissipative effects. The gas initially compressed by this infinitely strong shock wave is then isentropically expanded to a finite pressure. This would cause zero density at the wall. As pointed out in Section I, two other difficulties arise associated with the initial condition. This is peculiar to the problem in question and would give rise to a difficulty which is not encountered in the shock tube problem. It should also be mentioned here that Eqs. (1) to (5) do not include real gas effects which will influence the flow near the axis.

III. Numerical Simulations

A. *Random Choice Method*

Let Δr and Δt be increments of the variables r and t, respectively, where $\Delta r = R_0/N$; N being the number of meshes. Approximation of $\partial U/\partial t$ in Eq. (1) by the first-order difference quotient together with operator splitting leads to

$$\frac{U_j^* - U_j^n}{\Delta t} = -F_r(U_j^n) \tag{10}$$

and

$$\frac{U_j^{n+1} - U_j^*}{\Delta t} = -W(U_j^*), \tag{11}$$

where the subscript r denotes the partial differentiation with respect to r and

$$U_j^n = U(j\Delta r, n\Delta t). \tag{12}$$

Equation (10) suggests that the provisional value U_j^* is a solution of the plane flow problem. It is solved here by the random choice method. U_j^{n+1} is then obtained from Eq. (11) by a simple calculation. Preliminary calculations were made for the plane and cylindrical shock tube problems which had the initial pressure ratios of tens to thousands. Two methods of generating random numbers, i.e., the mixed congruential method proposed by Chorin [20] and the van der Corput method first adopted by Colella [21], were tested. The two results were nearly identical although the latter produced smoother and slightly better solutions. It was then decided to adopt the van der Corput sequence. The number of meshes N was first taken as 100. The scattering of the numerical points caused by the randomness of the sequence was noticeable. It was then taken as 1000 in the subsequent calculations. The increment of time Δt was determined by the Courant–Friedrichs–Lewy condition [22], which is written as

$$\Delta t < \Delta r/(|u| + c). \tag{13}$$

The condition of symmetry was used for the boundary condition at the wall $r = R_0$, that is,

$$p_{N-1/2} = p_{N+1/2}, \qquad \rho_{N-1/2} = \rho_{N+1/2}, \qquad u_{N-1/2} = -u_{N+1/2}, \tag{14}$$

where the suffix N indicates the mesh point on the wall. Zero density at the wall $r = R_0$ was replaced by a finite small value to get rid of the computational difficulty. If the numerical scheme is stable, then the error would eventually disappear. In fact several different values of density were tested but no appreciable changes appeared. At various time steps the global conservation of mass and energy has been checked by integrating the variables throughout the flow region. It has been proved that errors are not significant. The result of the final calculations is shown in Figs. 1 to 3 for $E_0 = 10$, 100, and 1000. The ratio of specific heats γ is assumed to be 1.4 as well as in the subsequent calculations. Nondimensional pressure $\bar{p}$, density $\bar{\rho}$, and particle velocity $\bar{u}$ are taken on the ordinate and $\bar{r} = r/R_0$ on the abscissa. These figures show the comparison of the spatial distribution of variables at various times as the solution develops. The times are taken such that the shock front is at $\xi = 0.3$, 0.6, and 0.9. The loci of the propagation of the shock front are shown in Fig. 4. The results obtained by the method of integral relations [3] are also shown in these figures. It is to be noted that the two results obtained by distinctly different numerical methods are nearly identical. This would imply the correctness of each solution. Figure 5 shows the relation among the pressure, particle velocity, and density at the shock front. The solid lines represent the Rankine–Hugoniot relations. It can be seen that the result of the random choice method satisfies the Rankine–Hugoniot relations with high accuracy. Figures 1 to 3 suggest that, as the

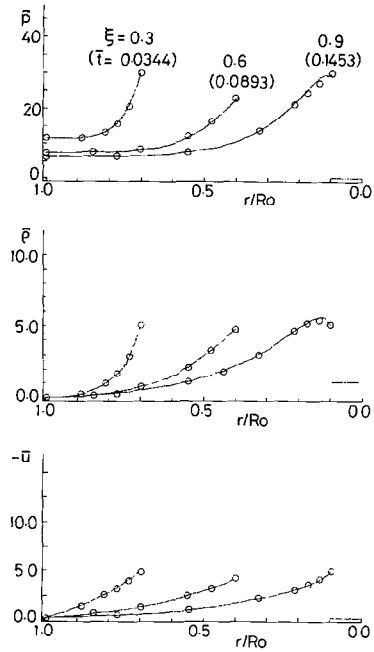

FIG. 1. Spatial distribution of pressure, density, and particle velocity, $E_0 = 10$: ---, random choice method; ○, method of integral relations.

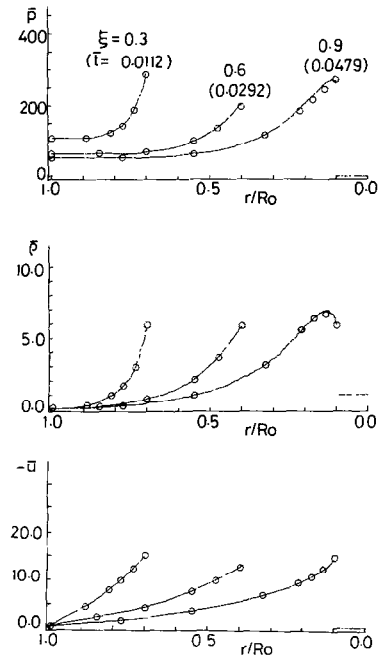

FIG. 2. Spatial distribution of pressure, density, and particle velocity, $E_0 = 100$: ---, random choice method; ○, method of integral relations.

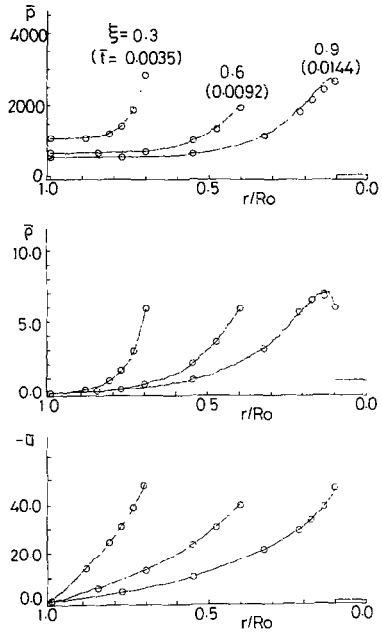

FIG. 3. Spatial distribution of pressure, density, and particle velocity, $E_0 = 1000$: ---, random choice method; ○, method of integral relations.

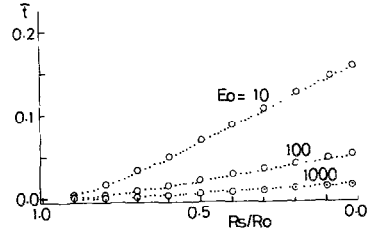

FIG. 4. Propagation loci of shock front, ---, random choice method: ○, method of integral relations.

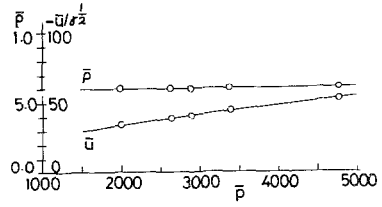

FIG. 5. Relation among pressure, density, and particle velocity at shock front, $E_0 = 1000$: —, Rankine–Hugoniot relations: ○, random choice method.

shock front approaches the axis, the two results begin to differ slightly from each other. To investigate this more closely, the behavior of the solutions is compared in the region near the axis in Figs. 6 to 8. Nondimensional variables $\bar{p}/M^2$, $\bar{\rho}$, and $\bar{u}/M$ are taken on the ordinates, where M is the propagation Mach number of the shock front referred to the sound speed c_0. A nondimensional space coordinate r/R_s is taken on the abscissa in place of r/R_0. In the random choice method, M is calculated using the Rankine–Hugoniot relation. It can be seen that the solutions obtained by the random choice method approach the selfsimilar solutions [5] more quickly than those obtained by the method of integral relations. In the previous study [3], it was suggested that the convergence of the method of integral relations tended to deteriorate as the shock front approached the region in close proximity to the axis. It might then be concluded that the random choice method would produce more exact solutions. This will be reaffirmed later by the result of the method of characteristics. Figures 6 to 8 also suggest that the rate of approach to the selfsimilar solution is faster for a larger value of E_0. The tendency is particularly noticeable in the density distribution. Figure 9 shows the plot of the pressure at the shock front against E_0 for fixed values of ξ. It can be seen that for various ξ (accordingly for various times) it is proportional to E_0 except for the cases of small E_0 ($E_0 < 20$). It also implies that the temperature and the particle velocity in strong

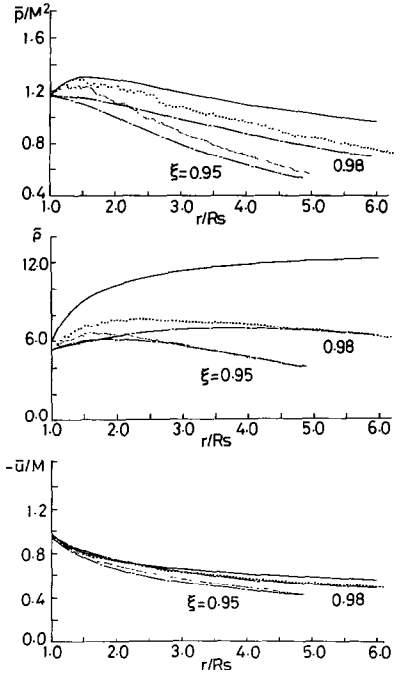

FIG. 6. Spatial distribution of pressure, density, and particle velocity in the focusing stage, $E_0 = 10$: —, selfsimilar solution: ---, random choice method: – – –, method of integral relations.

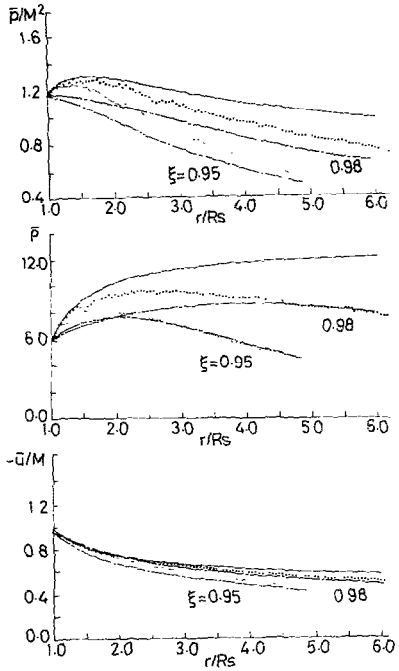

FIG. 7. Spatial distribution of pressure, density, and particle velocity in the focusing stage, $E_0 = 100$: —, selfsimilar solution; ---, random choice method; – – –, method of integral relations.

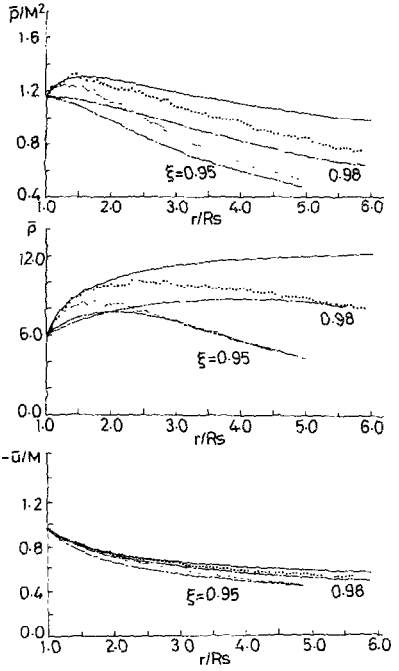

FIG. 8. Spatial distribution of pressure, density, and particle velocity in the focusing stage: $E_0 = 1000$: —, selfsimilar solution; ---, random choice method; – – –, method of integral relations.

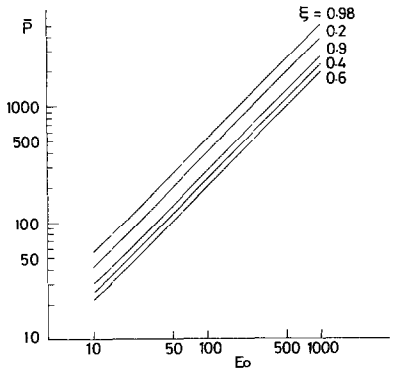

FIG. 9. Dependence of the pressure at the shock front upon the initiation energy E_0.

shocks near the axis are proportional to E_0 and $E_0^{1/2}$, respectively. The main features of the behavior of the solution near the axis are then enumerated as follows: (i) The solution tends to approach the selfsimilar implosion limit. However, the rate of approach is slower than expected. (ii) The selfsimilar solution begins to hold when the shock radius is less than 2% of the initiation radius ($\xi > 0.98$). Even then, it only holds in a region immediately behind the front, say in the region $r/R_s < 1.5$. (iii) The distribution of the particle velocity is closely approximated by the selfsimilar solution over a wide region behind the front. It is needless to say that this does not imply the validity of the selfsimilar solution. (iv) The rate of approach to the selfsimilar solution is faster for a larger value of E_0. The tendency is particularly noticeable in the density distribution. (v) The pressure and the temperature at the shock front are proportional to E_0 and the particle velocity to $E_0^{1/2}$ except for the cases of small E_0 ($E_0 < 20$).

B. *Method of Characteristics*

The objective of this section is to reaffirm the conclusion obtained in the preceding section. We shall put emphasis upon the behavior of the solution immediately behind the shock front. The method of characteristics is adopted to solve the same problem.

Characteristic forms of the conservation laws are approximated by finite difference equations as [23]:

$$\Delta_+ u + 2\Delta_+ c/(\gamma-1) = c\Delta_+ s/[\gamma(\gamma-1)c_v] - cu\Delta_+ t/r, \qquad \text{on} \quad C_+, \tag{15}$$

$$\Delta_- u - 2\Delta_- c/(\gamma-1) = -c\Delta_- s/[\gamma(\gamma-1)c_v] + cu\Delta_- t/r, \qquad \text{on} \quad C_-, \tag{16}$$

$$\Delta_0 s = 0, \qquad \text{on} \quad C_0, \tag{17}$$

where s is entropy and c_v is the specific heat at constant volume; Δ_+, Δ_-, and Δ_0

respectively represent the increments of variables along the characteristic curves C_+, C_-, and C_0 which are defined by

$$\Delta_+ r = (u+c)\,\Delta_+ t, \qquad \text{on} \quad C_+, \tag{18}$$

$$\Delta_- r = (u-c)\,\Delta_- t, \qquad \text{on} \quad C_-, \tag{19}$$

$$\Delta_0 r = u\Delta_0 t, \qquad \text{on} \quad C_0. \tag{20}$$

The system of equations, Eqs. (15) to (20), is sufficient for the calculation of interior points (the region behind the shock front). The Hartree's method [24] combined with the predictor-corrector method was used to solve it. In the region near the shock front, only one family of characteristics, either C_+ or C_-, overtakes the shock boundary from behind. Then only two equations, either Eqs. (15) and (18) or Eqs. (16) and (19), are usable. Three more equations are necessary to solve the problem. They are given by the Rankine–Hugoniot relations which hold on the shock boundary and are written as

$$u = c_0(1-\mu^2)(M - 1/M), \tag{21}$$

$$c = \sqrt{\gamma} c_0 \{[(1+\mu^2)\,M^2 - \mu^2][(1-\mu^2)/M^2 + \mu^2]\}^{1/2}, \tag{22}$$

$$s = c_v ln\{[(1+\mu^2)\,M^2 - \mu^2][(1-\mu^2)/M^2 + \mu^2]^{\gamma}\}, \tag{23}$$

where

$$\mu^2 = (\gamma - 1)/(\gamma + 1). \tag{24}$$

First assuming M, we can find the shock position P at the next time step. Then u, c, and s at P are calculated by Eqs. (21) to (24). The characteristic C_+ or C_- can be drawn through P. This determines the point of intersection Q on the initial line. Using Eq. (15) or Eq. (16), the value of s at P is recalculated; in this case the coefficients take the average between the values at P and Q. Compare the two values of s. Repeat this procedure until the desired accuracy is attained. As mentioned previously, the sound velocity is infinite at the wall. A finite large value is then assumed to get rid of this difficulty. As shown in the previous study [4], a singular characteristic C_s starts from the wall at an instant $t = t_0$ (corresponding, ξ is ξ_0) and overtakes the shock front at the instant of collapse (see Fig. 14 of Ref. [4]). If an initial line is chosen on which ξ is larger than ξ_0, then the section intercepted by C_s and the wall does not include the domain of dependence of the region between the shock front and C_s. Therefore, a small error in the initial data in the neighborhood of the wall has no influence upon the solution immediately behind the shock front. In fact, the calculation was started from a line $\xi = 0.3 > \xi_0$ with the initial data prescribed by the method of integral relations [3, 4]. The number of meshes N was taken as 1000. The increment of time Δt was determined by the Courant–Friedrichs–Lewy condition Eq. (13). It has been shown that the results agree well with those of the random choice method and the method of integral

relations in the various stages of the shock propagation except for the focusing stage. In particular, the propagation speeds and the variables at the shock front are everywhere identical. In the vicinity of the axis, the spatial distributions obtained by the method of integral relations begin to differ from two other solutions. Figure 10 shows the comparison among the three solutions near the axis. It is the same as Fig. 8 for the 0.98 case with the characteristic results added. The results of the random choice method and the method of characteristics are nearly identical and tend to approach the selfsimilar solutions more quickly. Considering the fact that the two methods are based on distinctly different formulations and that the convergence of the method of integral relations deteriorates in the focusing stage, it might be concluded that the random choice method and the method of characteristics produce correct solutions. It also suggests that the conclusion which has been deduced from the random choice method is correct.

C. *Finite Difference Methods*

It seemed that the situation associated with the initial conditions was particularly severe for the finite difference method. Several schemes were then tested with different artificial viscosities. Most of the calculations could not be rid of strong oscillation behind the discontinuity. They eventually led to instability. The most

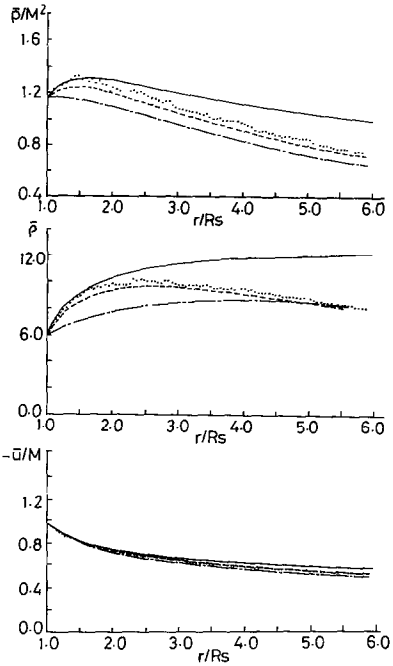

FIG. 10. Comparison of various methods, $E_0 = 1000$: spatial distribution of pressure, density, and particle velocity in the focusing stage $\xi = 0.98$; —, selfsimilar solution; ---, random choice method; — —, method of characteristics; – –, method of integral relations.

favorable result was obtained by the second-order schemes, particularly by the MacCormack scheme [19] with artificial diffusion terms $\mu\partial^2 U/\partial r^2$. The result of the calculation was, however, sensitive to the choice of the viscosity coefficient. The smallest value of the viscosity coefficient was chosen that suppressed the oscillation as small as possible. If the viscosity was too large, it noticeably smeared out the shock front. The viscosity coefficient determined in this way varied with the initial pressure ratio. The result of calculation agreed well with the other three results except for the region near the axis. In the focusing stage, it begins to differ from the others. The shock speed is slower and the discontinuity is smeared out due to viscosity. Small oscillations still remain behind the shock front. The comparison with the selfsimilar solutions is then difficult. Figure 11 shows an example of the results where it is compared with the result of the method of integral relations. The viscosity of Tyler's form [25] and the tensor viscosity proposed by Schultz [26] were also tested but stable solutions were not obtained. In the strict sense, a term $\mu\partial^2 U/\partial r^2$ does not represent the physical viscosity for cylindrical and spherical cases. It is then interesting to note that such an artificial viscosity only enables us to perform calculation. However, it should be finally mentioned that difficulties encountered here do not imply the deficiency of finite difference methods. Rather

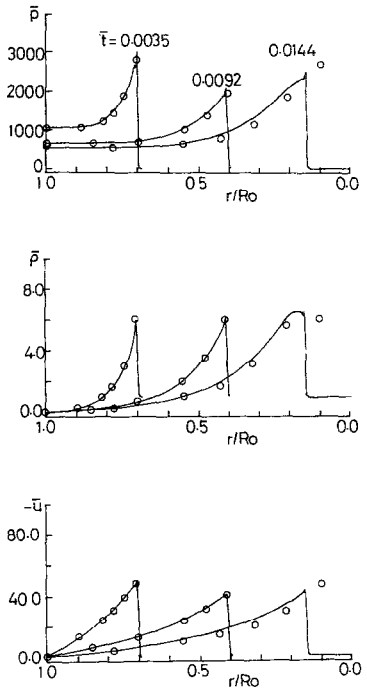

FIG. 11. Spatial distribution of pressure, density, and particle velocity, $E_0 = 1000$: MacCormack method compared with method of integral relations; —, MacCormack method; ○, method of integral relations.

more modern methods [9–12] as reviewed in Section I would produce solutions with higher accuracy.

In foregoing discussions, it has been pointed out that both the random choice method and the method of characteristics produce favorable results although the two methods are based on distinctly different formulations. However, unlike finite difference methods which rely on artificial viscosity for treating shocks, both the random choice method and the method of characteristics satisfy exact Rankine–Hugoniot relations (the random choice method possibly violates them in the process of operator splitting but numerical results have demonstrated that it actually satisfies the relations very exactly; see Fig. 5). Therefore their mutual success seems to indicate that the accuracy of computing converging shock waves depends predominantly on the accuracy in computing the shock itself, and to a lesser extent on the accuracy in computing the isentropic compression that follows the shock. Hence the agreement that has been demonstrated between the two methods is not expected to be universal. Rather, in flows with largely isentropic compression or rarefaction, one would generally expect the method of characteristics to be the superior one, since conservation of entropy along particle paths is directly incorporated into this method. (All that does not detract from the desirability of the random choice method, since it is far less complex in treating flow discontinuities than the method of characteristics.)

IV. Conclusion

The fluid flow caused by the propagation of a cylindrically converging shock wave is numerically simulated. The behavior of the solution in the focusing stage is investigated in detail and compared with the selfsimilar solution. The shock wave is assumed to be generated by an instantaneous energy release on a rigid cylindrical wall. Numerical methods such as the random choice method, the method of characteristics, and the second-order accurate finite difference method with artificial viscosities are adopted. The results are also compared with those of the method of integral relations. They all agreed well with one another except for the focusing stage. The random choice method and the method of characteristics produce nearly identical results in the focusing stage. The rate of approach to the selfsimilar solution is faster in these two methods than in the method of integral relations. It might then be concluded that the random choice method and the method of characteristics produce correct solutions. The finite difference method also produces identical results except for the focusing stage. In the focusing stage, the shock speed is slower and the discontinuity is smeared out due to viscosity. Small oscillations still remain behind the shock front. The comparison with the selfsimilar solution is then difficult. However, it might be expected that more modern numerical methods incorporating finite differences would improve the result. The main features of the behavior of the solution near the axis are enumerated as follows: (i) The solution tends to approach the selfsimilar implosion limit. However, the rate of approach is

slower than expected. (ii) The selfsimilar solution begins to hold when the shock radius is less than 2% of the initiation radius ($\xi > 0.98$). Even then, it only holds in a region immediately behind the front, say in the region $r/R_s < 1.5$. (iii) The distribution of the particle velocity is closely approximated by the selfsimilar solution over a wide region behind the front. However, this does not imply the validity of the selfsimilar solution. (iv) The rate of approach to the selfsimilar solution is faster for a larger value of the initiation energy E_0. The tendency is particularly noticeable in the density distribution. (v) The pressure and the temperature at the shock front are proportional to E_0 and the particle velocity to $E_0^{1/2}$ except for the cases of small $E_0 (E_0 < 20)$.

REFERENCES

1. G. G. BACH AND J. H. LEE, *J. Fluid Mech.* **37**, 513 (1969).
2. H. MATSUO, *Mem. Fac. Eng. Kumamoto Univ.* **23**, 1 (1977).
3. H. MATSUO, *Phys. Fluids* **22**, 1618 (1979).
4. H. MATSUO, *Phys. Fluids* **26**, 1755 (1983).
5. G. GUDERLEY, *Luftfahrtforschung* **19**, 302 (1942).
6. R. A. ROIG AND I. I. GLASS, *Phys. Fluids* **20**, 1651 (1977).
7. H. MATSUO, K. EBIHARA, Y. OHYA, AND H. SANEMATSU, *J. Appl. Phys.* **58**, 2487 (1985).
8. H. MATSUO, K. EBIHARA, Y. OHYA, AND K. FUJIWARA, *Appl. Phys. Lett.* **49**, 443 (1986).
9. P. L. ROE, *Annu. Rev. Fluid Mech.* **18**, 337 (1986).
10. A. HARTEN, *J. Comput. Phys.* **49**, 357 (1983).
11. P. L. ROE AND J. PIKE, *Computing Methods in Applied Sciences and Engineering, VI*, edited by R. Glowinski and J. L. Lions (North-Holland, Amsterdam, 1984).
12. M. BEN-ARTZI AND J. FALCOVITZ, *SIAM J. Sci. Statist. Comput.* **7**, 744 (1986).
13. G. A. SOD, *J. Fluid Mech.* **83**, 785 (1977).
14. J. GLIMM, *Commun. Pure Appl. Math.* **18**, 697 (1965).
15. T. SAITO AND I. I. GLASS, *Proc. R. Soc. London A* **384**, 217 (1982).
16. R. B. PAYNE, *J. Fluid Mech.* **2**, 185 (1957).
17. A. LAPIDUS, *J. Comput. Phys.* **8**, 106 (1971).
18. S. ABARBANEL AND M. GOLDBERG, *J. Comput. Phys.* **10**, 1 (1972).
19. R. W. MACCORMACK, *AIAA Paper 69-354*, 1969.
20. A. J. CHORIN, *J. Comput. Phys.* **22**, 517 (1976).
21. P. COLELLA, Lawrence Berkely Laboratory Rep. LBL-8774, 1979 (unpublished).
22. R. D. RICHTMYER AND K. W. MORTON, *Difference Methods for Initial-value Problems* (Interscience, New York, 1967), Chap. 12, p. 304.
23. R. COURANT AND K. O. FRIEDRICHS, *Supersonic Flow and Shock Waves* (Interscience, New York, 1967), Chap. 3, p. 202.
24. D. R. HARTREE, *Numerical Analysis* (Oxford Univ. Press, London, 1958).
25. L. D. TYLER, in *Proceedings of the Second International Conference on Numerical Methods in Fluid Dynamics*, Lecture Notes in Physics Vol. 8 (Springer, New York, 1971).
26. W. D. SCHULZ, *J. Math. Phys.* **5**, 133 (1964).